

# Function reconstruction as a classical moment problem: A maximum entropy approach

Parthapratim Biswas

*Department of Physics and Astronomy, The University of Southern Mississippi, Hattiesburg, MS 39406, USA\**

Arun K. Bhattacharya

*Department of Physics, The University of Burdwan, Burdwan, WB 713104, India*

We present a systematic study of the reconstruction of a non-negative function via maximum entropy approach utilizing the information contained in a finite number of moments of the function. For testing the efficacy of the approach, we reconstruct a set of functions using an iterative entropy optimization scheme, and study the convergence profile as the number of moments is increased. We consider a wide variety of functions that include a distribution with a sharp discontinuity, a rapidly oscillatory function, a distribution with singularities, and finally a distribution with several spikes and fine structure. The last example is important in the context of the determination of the natural density of the logistic map. The convergence of the method is studied by comparing the moments of the approximated functions with the exact ones. Furthermore, by varying the number of moments and iterations, we examine to what extent the features of the functions, such as the divergence behavior at singular points within the interval, is reproduced. The proximity of the reconstructed maximum entropy solution to the exact solution is examined via Kullback-Leibler divergence and variation measures for different number of moments.

PACS numbers: 02.30.Zz, 05.10.-a, 02.60.Pn

## I. INTRODUCTION

The reconstruction of a non-negative distribution from its moments constitutes the so-called classical moment problem, and is an archetypal example of an inverse problem [1, 2] in mathematical sciences. Owing to its importance in the context of probability theory and the challenging problems of analysis associated with it, the moment problem has attracted the attention of a large number of researchers from many diverse fields of science and engineering [3–13]. In the classical Hausdorff moment problem (HMP), one addresses the problem of reconstructing a non-negative, real valued function  $f(x)$  in a finite interval  $[a, b]$  from a sequence of real numbers. The sequence forms a ‘moment sequence’ that satisfies the Hausdorff conditions [14]. The problem is severely ill-posed in the Hadamard sense [15]. For a finite number of moments, most of the existing numerical methods are susceptible to large instabilities but several methods do exist that attempt to construct a regularized solution by avoiding these instabilities [9, 16]. The HMP has been addressed by using a variety of methods (such as Tikhonov’s regularization method [17] and the use of Pollaczek polynomial by Viano [18, 19]) but the information-theoretic approach is particularly fascinating to the physicists. The latter is based on the *maximum entropy principle* (MEP) proposed by Jaynes [20]. The MEP provides a suitable framework to reconstruct a distribution by maximizing the Shannon information entropy [21] and at the same time ensures the matching

of the moments of the distribution. Our interest in the moment problem stems from the fact that inverse problems of this type are frequently encountered in many areas of physical, mathematical and biological sciences [5–12, 22, 23]. A very simple but elegant example is the inversion of the specific heat data of solids. It is known that the constant volume vibrational specific heat of a solid can be expressed as the convolution of a known function of the frequency and the vibrational frequency distribution function (FDF) [24]. The task of extracting the FDF by inverting the experimentally-measured values of the specific heat at constant volume as a function of temperature is a well-known example of an inverse problem in solid state physics [25, 26].

The focus of our present work is to reconstruct a non-negative function very accurately within the framework of the MEP from the knowledge of a finite number of moments. Although there exists a number of numerical procedures that address this problem, most of them become unreliable when the number of moment constraints exceeds a problem-dependent upper limit. A close review of the methods and the study of the example functions presented therein immediately reveal the weakness of the methods [9, 16]. For example, it is very difficult to reproduce accurately the van Hove singularities in the frequency distribution of (crystalline) solids or the presence of a gap in the density of electronic states in a solid. While the algorithm proposed by Silver and Röder [27] does reproduce the latter correctly and is capable of dealing with a large number of moments, we are not aware of any systematic study of function reconstruction by this approach at this time. It is, therefore, worthwhile to explore the possibility of developing a reliable scheme for the entropy optimization program and to apply it to a

---

\*Electronic address: Partha.Biswas@usm.edu

range of non-negative functions having complex structure within the interval.

The rest of the paper is organized as follows. In Section II we briefly describe a procedure that has been developed recently by us to reduce the moment problem to a discretized entropy optimization problem (EOP) [28]. We then test our methodology in Section III by examining to what extent it is successful in reconstructing a wide variety of functions on the basis of input information in the form of Chebyshev moments of the functions. The convergence behavior of the maximum entropy solution is then discussed in Section IV with particular emphasis on the number of moments. The proximity of the reconstructed solution to the exact solution for different distributions is also studied via Kullback-Leibler [29] divergence and variation measures [30].

## II. MAXIMUM ENTROPY APPROACH TO THE HAUSDORFF MOMENT PROBLEM

The classical moment problem for a finite interval  $[a, b]$ , also known as the Hausdorff moment problem [14], can be stated as follows. Consider a set of moments

$$\mu_i = \int_a^b x^i \rho(x) dx \quad i = 0, 1, 2, \dots, m, \quad i \leq m \quad (1)$$

of a function  $\rho(x)$  integrable over the interval with  $\mu_i < \infty \forall x \in [a, b]$ . The problem is to construct the non-negative function  $\rho(x)$  from the knowledge of its moments. The necessary and sufficient conditions for a solution to exist were given by Hausdorff [14]. The moment problem and its variants have been studied extensively in the literature [1, 2, 18, 22, 31]. Mead and Papanicolaou [9] have, in particular discussed a number of moment problems encountered in various of physics. For a finite number of moments, the problem is underdetermined and it is not possible to construct the unique solution from the moment sequence unless further assumptions about the function are made. Within the framework of maximum entropy principle, one attempts to find a function  $\rho(x)$  that maximizes the information entropy functional,

$$S[\rho] = - \int_a^b \rho(x) \ln[\rho(x)] dx \quad (2)$$

subject to the moment constraints defined by Eq. (1). The resulting solution is an approximate function  $\rho_{ME}(x)$ , which can be obtained by functional differentiation of a Lagrangian with respect to the unknown function  $\rho(x)$ . The Lagrangian is given by,

$$L(\rho, \lambda) = -S[\rho] + \sum_{i=0}^m \lambda_i \left( \int_a^b x^i \rho(x) dx - \mu_i \right). \quad (3)$$

Now,

$$\frac{\delta L}{\delta \rho(x)} = 0 \implies \rho_{ME}(x) = \exp \left( - \sum_{i=0}^m \lambda_i x^i \right). \quad (4)$$

The normalized function  $\rho(x)$  is often referred to as probability density since it is positive semidefinite and the interval  $[a, b]$  can be mapped onto  $[0, 1]$  without any loss of generality. For a normalized function with  $\mu_0 = 1$ , the Lagrange multiplier  $\lambda_0$  is connected to the others via,

$$e^{\lambda_0} = \int_0^1 \exp \left( - \sum_{i=1}^m \lambda_i x^i \right) dx = Z,$$

and the maximum entropy (ME) solution can be written as,

$$\rho_{ME}(x) = \exp \left( - \sum_{i=1}^m \lambda_i x^i \right) / Z, \quad (5)$$

where  $Z$  is known as the partition function.

A reliable scheme for handling the entropy optimization problem subject to the matching of the moments was discussed by us in Ref. [28]. The essential idea behind the approach is to use a discretized form of the Shannon entropy functional and the moment constraints using an accurate quadrature formula. The constraint optimization problem involving the primal variables is then reduced to an unconstrained convex optimization program involving the dual variables of the problem. This guarantees the existence of a unique solution within the framework of maximum entropy principle. The solution is *least biased* [32] and satisfies the moment constraints defined by Eq. (1). The procedure consists of: 1) rewriting the Lagrangian of the problem in Eq. (3) in terms of the discretized variables to obtain the ME solution, 2) using the resulting ME solution in association with Eq. (1) to reduce the EOP as an unconstrained convex optimization problem in dual variables, and finally 3) minimizing the objective function in the dual space to obtain the optimal solution in the primal space.

Using a suitable quadrature (e.g. Gaussian) with a set of weights  $\omega_j$ 's and abscissae  $x_j$ 's, the discretized Lagrangian can be written as,

$$L(\tilde{\rho}, \tilde{\lambda}) = \sum_{j=1}^n \tilde{\rho}_j \ln \left( \frac{\tilde{\rho}_j}{\omega_j} \right) - \sum_{i=1}^m \tilde{\lambda}_i \left( \sum_{j=1}^n t_{ij} \tilde{\rho}_j - \mu_i \right), \quad (6)$$

where  $0 \leq \tilde{\rho} \in R^n$  and  $\tilde{\lambda} = -\lambda \in R^m$ , respectively are the primal and the dual variables of the EOP. In the equation above, we have used the notation  $\tilde{\rho}_j = \omega_j \rho_j$  and  $t_{ij} = (x_j)^i$ . The discretized ME solution is given by the functional variation with respect to the unknown function as before,

$$\rho_j^{ME} = \exp \left( \sum_{i=1}^m t_{ij} \tilde{\lambda}_i - 1 \right), \quad j = 1, 2, \dots, n. \quad (7)$$

Equations (1) and (7) can be combined together and the EOP can be reduced to an unconstrained convex op-

timization problem involving the dual variables  $\tilde{\lambda}$ 's:

$$\min_{\tilde{\lambda} \in R^m} \left[ D(\tilde{\lambda}) \equiv \sum_{j=1}^n \omega_j \exp \left( \sum_{i=1}^m t_{ij} \tilde{\lambda}_i - 1 \right) - \sum_{i=1}^m \mu_i \tilde{\lambda}_i \right]. \quad (8)$$

By iteratively obtaining an estimate of  $\tilde{\lambda}$ ,  $D(\tilde{\lambda})$  can be minimized, and the ME solution  $\tilde{\rho}(\tilde{\lambda}^*)$  can be constructed from Eq. (7). The objective function  $D(\tilde{\lambda})$  can be minimized by modifying a method, which is largely due to Bergman [33], and was presented and discussed at length in Ref. [28] both for the power and the Chebyshev moments. For the latter, the ME solution can be shown to be expressed in the form of Eq.(7) with  $t_{ij} = T_i^*(x_j)$ , where  $T_i^*(x)$  is the shifted Chebyshev polynomials. In the following, we apply our algorithm to reconstruct a variety of functions corresponding to different number of shifted Chebyshev moments.

### III. APPLICATION TO FUNCTION RECONSTRUCTION

We now illustrate the method by reconstructing a number of exact functions from a knowledge of their moments. For all but one of the examples studied here, the moments of the functions can be obtained from analytical expressions. In the remaining case the moments have been calculated numerically using standard double precision arithmetic. As mentioned earlier, we map the functions onto the interval  $[0,1]$  and assume they are normalized so that the functions can be treated as probability density functions (pdf) without any loss of generality. It is well-known that for a finite number of moments, the Hausdorff moment problem cannot be solved uniquely. One needs to supply additional information to choose a suitable solution from an ensemble of solutions that satisfy the given moment constraints. The maximum entropy (ME) ansatz constructs the *least biased* solution that maximizes the entropy associated with the density and is consistent with the given moments. The accuracy of the reconstructed solution can be measured by varying the number of moments. A comparison with the exact solution (if available) would reveal to what extent the ME solution matches with the exact solution. For an unknown function with a finite set of moments, the quality of the ME solution may be judged by the proximity of the input (exact) moments to the output (approximated) moments resulting from the reconstructed distribution. By increasing the number of moments one can systematically improve the quality of the solution. It should, however, be noted, that for a function with a complicated structure, the convergence of the first few moments does not guarantee its accurate reproduction. The ME solution in this case may not represent the exact solution, but is still correct as far as the maximum entropy principle is concerned. It is therefore important to study the convergence behavior of the solutions with

moments for a number of functions with widely different shapes. To this end we compare, in the following, our maximum entropy solution corresponding to a variety of exact distribution and a distribution amenable to an accurate numerical analysis.

#### A. Case 1 : $f(x) = 1$

We begin with a step function which is unity throughout the interval  $[0, 1]$ . As mentioned earlier, we use the shifted Chebyshev polynomials  $T_n^*(x)$ , which is defined via,

$$\begin{aligned} T_n^*(x) &= T_n(2x - 1) \\ T_n(x) &= \cos [n \cos^{-1}(x)] \quad \text{for } n = 0, 1, \dots \end{aligned}$$

The moments can be calculated analytically in this case, and are given by,

$$\mu_0 = 1; \quad \mu_1 = 0; \quad \mu_n = \frac{1 + (-1)^n}{2 - 2n^2} \quad n \neq 1.$$

Although the function does not have any structure, it is particularly important because of its behavior at the end points. Owing to the presence of discontinuities at  $x = 0$  and  $1$ , the function is difficult to reproduce close to these points. The sharp discontinuities cause the reconstructed function (from a small number of moments) to exhibit spurious oscillations near the end points. The oscillations are progressively suppressed by increasing the number of Chebyshev moments in our iterative method. Beyond 100 moments the oscillations completely disappear. This behavior is seen clearly in fig.1 where we have plotted the reconstructed functions corresponding to 40, 60 and 80 moments. The oscillations are particularly pronounced as one approaches  $x = 1$ , but die down with increase in the number of moments. The result corresponding to 100 moments is presented in fig.2. The plot clearly reveals that the function has been reproduced with an error, which is less than 1 part in  $10^6$ .

#### B. Case 2 : $f(x) = \frac{3}{2}x^{\frac{1}{2}}$

The next example we consider is a square-root function  $f(x) = \frac{3}{2}x^{\frac{1}{2}}$ , where the prefactor is chosen to normalize the function. In many physical problems, we often encounter distributions showing a square-root behavior. For example, the spectral distribution of a free electron gas in 3-dimension is related to the energy via  $\sqrt{E}$ , and the square-root behavior persists in the weak interaction limit (at low energy). It is therefore important to see if such a square-root function can be reproduced with a high degree of accuracy using our maximum entropy ansatz. The shifted Chebyshev moments for the present case are given by,

$$\mu_n = \frac{9 - 12n^2}{9 - 40n^2 + 16n^4} \quad \text{for } n \geq 0.$$

The results for the function are plotted in figs. 3 to 5 for 100 moments. The reconstructed function is found to match excellently with the exact function throughout the interval as shown in fig.3. Of particular importance is the behavior of the function near  $x = 0$  and 1. The square-root behavior is accurately reproduced without any deviation or oscillation near  $x = 0$  as is evident from fig.4. Similarly, the behavior near  $x = 1$  is also reproduced with a high degree of accuracy as shown in fig.5. Since our method can exploit the information embedded in the higher moments, it is capable of reproducing the function very accurately without any oscillation.

### C. Case 3: A double-parabola with a gap

Having discussed two relatively simple examples, we now consider a case where the function vanishes in a finite domain within the interval. Such a function appears frequently in the context of the energy density of states of amorphous and crystalline semiconductors. It is instructive to study whether our maximum entropy (ME) method is capable of reproducing a gap in the energy eigenvalue spectrum. Since the moments of the electronic density of states can be obtained from the Hamiltonian of the system, our method can be used as an alternative tool to construct the density of states from the moments. This is particularly useful for treating a large non-crystalline system (e.g. in the amorphous or liquid state), in which case the direct diagonalization of the Hamiltonian matrix is computationally overkill and scales with the cubic power of the system size. In contrast, our maximum entropy ansatz provides an efficient and accurate procedure for the determination of total (band) energy and the Fermi level subject to the availability of the energy moments. Here we use a toy model of a density of states that consists of two parabolae separated by a gap to illustrate the usefulness of our method. In particular, we choose a normalized distribution with a gap from  $x_1$  to  $x_2$ ,

$$f(x) = \begin{cases} Ax(x_1 - x) & \text{for } x \leq x_1 \\ B(x - x_2)(1 - x) & \text{for } x \geq x_2, \end{cases}$$

where A and B are given by

$$A = \frac{6}{x_1^2(1 + x_1 - x_2)}; \quad B = \frac{6}{(1 - x_2)^2(1 + x_1 - x_2)}.$$

In the present case, we choose  $x_1 = \frac{2}{5}$  and  $x_2 = \frac{3}{5}$  giving the value of the gap  $(x_2 - x_1) = \frac{1}{5}$ . The Chebyshev moments of the function can be calculated exactly, and as in

the previous examples the function is reconstructed from the moments. In figs. 6 and 7 we have plotted the results obtained from our ME ansatz along with the exact functional values at the quadrature points. It is remarkable to note that the reconstructed function matches excellently with the exact one. Furthermore, the method reproduces the gap between the parabolae correctly without any oscillation in the gap. Table 1 lists the size of the gap corresponding to different number of moments for two sets of Gaussian points. Since we are using a finite number of quadrature points, the accuracy of our gap size is limited by the resolution of the (non-uniform) quadrature grid near the gap. We have chosen a tolerance  $\epsilon = 5.0 \times 10^{-3}$  for the reconstructed functional value to locate the onset of the gap (i.e. the zero of the function) [34]. It is evident from table 1 that as the number of moments increases, the size of the gap improves and eventually converges very close to the exact numerical value. The accuracy can be improved further by using more Gaussian points in the quadrature.

TABLE I: Numerical values of the gap for different number of moments from the reconstructed double-parabolic distribution.

| Moments         | 96 points | 192 points |
|-----------------|-----------|------------|
| 20              | 0.1622    | 0.1676     |
| 40              | 0.1813    | 0.1875     |
| 60              | 0.1821    | 0.1902     |
| 80              | 0.1823    | 0.1909     |
| 100             | –         | 0.1922     |
| Exact numerical | 0.1941    | 0.1945     |

### D. Case 4: $f(x) = \frac{1}{\pi\sqrt{(x-x^2)}}$

We now consider a function that has singularities in the range  $[0,1]$ . For the purpose of our discussion we refer to this function as ‘U-function’ hereafter. The shifted Chebyshev moments of the function have the interesting property that except for the zeroth moment, all the other moments are identically zero. The task of the ME algorithm in this case is to construct a function having all the moments zero except for the zeroth moment, which is unity by normalization. It may be noted that the electronic density of states per atom  $D(E)$  of an infinite chain with a nearest neighbor interaction can be expressed in the form,

$$D(E) = \frac{1}{\pi} \frac{1}{\sqrt{4\beta^2 - (E - \alpha)^2}},$$

where  $\alpha$  and  $\beta$  are the on-site and the nearest neighbor hopping integrals respectively. The zeroth moment

is unity, which implies that there is only one state associated with each atom. For  $\alpha = 0$  and  $\beta = \frac{1}{2}$ , the density of states can be mapped onto the U-function within the interval  $[0:1]$ , and our algorithm can be applied to reconstruct the latter. An important characteristic of the density of states (or distribution function) is that it diverges at the band edges (or at the end points). Since all the Chebyshev moments are zero aside from the zeroth moment, it is important to see if the algorithm is capable of generating the density with the correct diverging behavior at the (band) edges. In fig.8 we have plotted the results for the function for three different sets of moments  $M = 10, 40,$  and  $80$  to illustrate how the approximate solutions improve with the increase of the number of moments. The shape of the function begins to emerge correctly even for as few as first 10 moments but with significant oscillations and poor divergence behavior near the end points. As the number of moments increases, the solution rapidly converges and the oscillations begin to disappear. In fig.9 we have plotted the results for  $M = 120$ . The reconstructed function matches excellently throughout the interval with the exact one. The behavior of  $f(x)$  near the left edge at  $x = 0$  is shown in fig.10 from  $x=0$  to  $x=0.05$ . It is evident from the plot that even for very small values of  $x$  near the left edge, the reconstructed values agree with the exact values excellently. A similar behavior has been observed near the right edge of the band near  $x=1$ . The capability of our method in reconstructing a function with singularities in the interval is thus convincingly demonstrated.

### E. Case 5: A function with a finite discontinuity

The functions that we have discussed so far in the examples above are continuous within the interval. It would be interesting to consider a case where the function has a finite discontinuity within the interval. As an example, we choose a double-step function,

$$f(x) = \begin{cases} \frac{1}{2} & \text{for } x \leq x_1 \\ \frac{3}{2} & \text{for } x \geq x_1, \end{cases}$$

which has a finite discontinuity at  $x_1 = \frac{1}{2}$ . It is rather challenging to reconstruct the function from the moments so that the local behavior near the discontinuity at  $x = 1/2$  is correctly reproduced. As before, the moment integrals can be calculated analytically in this case. In fig.11 we have plotted the function for 10, 20 and 50 moments. The solutions for the first two sets are expected to be less accurate, and indeed they show significant oscillations in the figure. For 50 moments the match is quite impressive. On adding further moments, the solution progressively improves. Figure 12 shows the remarkable accuracy with which the function is reproduced by employing the first 100 moments. An important

feature of the reconstructed function is that the discontinuity has been correctly reproduced with the exception of two points. From the various cases studied so far, we conclude that about 80 to 120 moments are needed for point-wise matching of the exact and the reconstructed functions.

### F. Case 6 : An unknown density

Up until now, we have considered cases where the exact form of the function is known. In practical problems, however, it is more likely that the exact function is not available. We should therefore consider a case where the analytical expression for the distribution is not known, but a direct numerical solution is possible. As an example of such a distribution, we choose the natural invariant density of the logistic map  $g(x) = \Gamma x(1-x)$  with  $\Gamma = 3.6785$ . The invariant density for the map can be obtained by calculating the moments from the time evolution of an ensemble of initial iterates  $x_0$  as discussed in Ref. [35]. Since the map is ergodic for this value of  $\Gamma$ , the moments obtained via the time evolution of the map are identical to the moments of the natural invariant density [23, 35]. The task of our maximum entropy algorithm is to reconstruct the approximate density, and to compare it with the numerical density. The latter can be obtained from a histogram of the iterates and averaging over a large number of configurations [35]. The result from our ME ansatz using the first 80 moments is plotted in fig.13 along with the numerical density. The plot clearly demonstrates that every aspect of the fine structure of the numerical density is reproduced excellently in the maximum entropy solution.

Finally, we end this section considering a rapidly oscillatory function having complex structure within the interval  $[0,1]$ . An example of such a function can be constructed as,

$$f(x) = \frac{1}{4}(\sin(167x) + \cos(73x)) + 6(x - \frac{1}{2})^2 + \frac{1}{2} \quad (9)$$

where the prefactors are chosen to normalize the function. In the context of studying diffusion in a rough one-dimensional potential, Zwanzig has studied such a function to obtain a general expression for the effective diffusion coefficient by analyzing the mean first-passage time [36]. The maximum entropy construction of this function is plotted in fig.14 for 90 moments along with the exact function. Once again the function is reproduced excellently with every little details of the local minima and maxima of the function.

## IV. CONVERGENCE BEHAVIOR OF THE RECONSTRUCTED SOLUTION

The convergence behavior of the maximum entropy solution has been discussed at length in the litera-

ture [29, 30, 37, 38]. The analytical efforts are particularly focused on constructing bounds of the proximity of the reconstructed density to the exact density assuming that a given number of moments of the distributions are identical. In particular, given a target distribution  $f(x)$  and a reconstructed distribution  $f_M(x)$  that have identical first  $M$  moments  $\mu_0 = 1, \mu_1, \dots, \mu_M$ , the proximity of the two distributions can be expressed via the Kullback-Leibler divergence [29] and the variation measure [30],

$$D_{KL}[f, f_M] = \int_S f(x) \ln \left( \frac{f(x)}{f_M(x)} \right) dx \quad (10a)$$

$$D_v[f, f_M] = \int_S |f_M(x) - f(x)| dx, \quad (10b)$$

where  $S$  is the support of the densities  $f(x)$  and  $f_M(x)$ . The divergence measure is also known as the relative entropy or information discrimination, and  $D_{KL} \geq 0$  with the equality holding if and only if  $f(x) = f_M(x)$  for all  $x$ . A lower bound for the divergence measure  $D_{KL}$  in terms of the variation measure was given by Kullback [39]:

$$D_{KL} \geq \frac{D_v^2}{2} + \frac{D_v^4}{12}, \quad (11)$$

where it was assumed that the first  $M$  moments are identical for both the distributions. Since the exact distributions are known for the examples considered here (except for the case 6), we can use these measures to examine if the reconstructed solution indeed satisfies the inequality. To this end, we first study the convergence of the moments of the reconstructed distributions with iteration and establish that the moments can be matched very accurately so that for practical purposes the reconstructed moments can be taken as identical to the exact (input) moments for the calculation of measure in Eqs. (10a) and (10b).

#### A. Convergence with respect to the number of iteration

As mentioned earlier, we have observed that the quality of the ME solutions depend on two factors: 1) the number of iterations and 2) the number of moments used for the purpose of reconstruction. In general, for a distribution with a fine structure, it is difficult to determine the minimal number of moments that are needed to reconstruct the function accurately. However, by studying a number of distributions with varying complexities and their convergence behavior, it is possible to obtain some useful information about the rate of convergence. We address this issue by choosing the U-function (case 4) as an example, but the observation is found to be true for other cases as well. For a systematic study of convergence behavior of the reconstructed moments with iterations, one requires a measure of the goodness of the fit. We therefore introduce  $\Delta_1$ , the root mean square (RMS) deviation

of the exact moments from the moments provided by the ME solution,

$$\Delta_1(N, M) = \sqrt{\frac{1}{M} \sum_{i=1}^M (\mu_i - \tilde{\mu}_i(N, M))^2}. \quad (12)$$

Here  $\mu$  and  $\tilde{\mu}(N, M)$  respectively denote the exact (or input) and the reconstructed (or output) moments, and the latter depends on the number of moments ( $M$ ) and the iteration number ( $N$ ). In the context of our present study, the exact moments of the functions are known, but in many practical cases they may not be available and need to be replaced by the input moments available for the problem. The quantity  $\Delta_1$  provides a measure of the proximity of the first  $M$  reconstructed moments to the exact ones, and a small value of  $\Delta_1$  is indicative of the fact that the moment constraints are satisfied with a high degree of accuracy. The value of  $\Delta_1$  becomes as small as  $10^{-14}$  provided an adequate number of iterations are performed to match a given set of moments. In fig.15, we have plotted  $\Delta_1$  for the case of U-function with the number of iteration progressively increasing to  $N = 6 \times 10^6$ . The RMS deviation decreases rapidly with the number of iteration and eventually drops to a value of the order of  $10^{-14}$ . An examination of the data suggests that  $\Delta_1$  can be fitted to an exponential decay with iteration and is plotted in fig.15. This behavior is also observed for the other distributions discussed in Section 3. It thus follows that the algorithm converges quite rapidly, and that the moment constraints can be satisfied to a high degree of accuracy even for a very large moment set.

#### B. Convergence with respect to the number of moments

While  $\Delta_1$  provides a measure of the goodness of the fit for the moments, it does not necessarily guarantee a point-wise convergence of the reconstructed function with the exact one. This is particularly true if a small number of moments are used to reconstruct the function that has a fine structure in it (cf. fig.13). In this case, the reconstructed moments can be matched to a high degree of accuracy with input moments, but the solution may still miss out the characteristic feature of the distribution folded in the higher order moments. The maximum entropy solution in this case may not reproduce the actual solution even though the approximate moments are very close to the exact moments. To ensure that  $\Delta_1$  indeed attains a sufficiently small value, we need to study the approximate solution vis-a-vis the number of moments for a fixed cycle of iterations. Since the exact functions are known in our cases, the simplest way to measure the quality of the ME solution is to construct the RMS deviations of the reconstructed functions from the exact ones

in the interval  $[0,1]$ :

$$\begin{aligned} \Delta_2(N, M) &= \sqrt{\frac{1}{n_g} \sum_{i=1}^{n_g} [f_i - \tilde{f}_i(N, M)]^2} \quad (13) \\ &\approx \Delta_2(M) \quad \text{for large } N, \end{aligned}$$

where  $n_g$  is the number of points used in the quadrature. Here we have assumed that the dependence of  $\Delta_2$  on  $N$  can be neglected so that  $\tilde{f}_i(N, M) \approx \tilde{f}_i(M)$ , which holds for large  $N$  owing to the fast decay of  $\Delta_1$ . We choose  $\Delta_1 = 10^{-15}$  for each of the moment sets to study the variation of  $\Delta_2(M)$  for different values of  $M$ . In practice, the exact function may not be available but the expression for  $\Delta_2$  can still be used by replacing the exact function  $f_i$  by  $\tilde{f}_i(M + \Delta M)$  and constructing the RMS deviation for increasing values  $M$  and  $\Delta M$ . In fig.16, we have plotted  $\Delta_2$  for the case of U-function for different values of  $M$ . The plot shows a monotonic decrease of  $\Delta_2$  with the increasing values of  $M$ . For this function, we see that a value of  $M=100$  to 120 provides a small enough  $\Delta_2$  to reconstruct the function accurately when  $\Delta_1 = 10^{-15}$ . The solid line in the figure is an exponential fit to the data indicating a fast convergence of our algorithm with respect to the moments for a fixed value of  $\Delta_1$ .

The proximity of the reconstructed distribution to the exact one can be quantified in terms of the divergence measure and the variation distance as defined in the beginning of this section. A number of inequalities can be found in the literature [30, 38] that provide lower bounds of the relative entropy. The inequality in (11) is an example of such a bound although still sharper bounds are available in the literature [30, 38]. In fig.17 we have plotted the relative entropy of the U-function for different number of moments. The reconstructed solution for each of the moment sets  $M$  corresponds to  $\Delta_1 = 10^{-15}$  so that the first  $M$  moments of the exact and the reconstructed functions are practically identical to each other. The right hand side of the inequality (11) is also plotted in the same figure for comparison. As the reconstructed solution approaches the exact solution with increasing number of moments, the relative entropy or information discrimination between the two distributions decreases and eventually comes very close to the analytically predicted lower bound.

## V. CONCLUSION

In this paper we study the reconstruction of functions from a set of Chebyshev moments (of the functions) via

maximum entropy optimization. The method consists of mapping the original constraint optimization problem in primal space onto an unconstrained convex optimization problem in the dual space by using a discretized form of the moments and the Shannon entropy of the function to be reconstructed. The resulting optimization problem is then solved iteratively by obtaining the optimal set of Lagrange's parameters as prescribed in Ref.[28]. By virtue of its ability to deal with a larger number of moments, our present approach is extremely robust and accurate. This makes it possible to reconstruct a variety of function that are difficult to handle otherwise.

We demonstrate the accuracy of this method by applying to a number of functions for which the exact moments are available. The method accurately reproduces not only smooth and continuous functions (such as square-root and double-parabolic functions) but also non-smooth and discontinuous functions (such as a double-step function with a finite discontinuity). It also captures the fine structure in a rapidly oscillatory function of known analytical form and the invariant densities of a logistic map corresponding to special values of the control parameter for which no analytical results are available. A convergence study of the reconstructed moments suggests that the RMS deviation of the moments (from the exact ones) can be made as small as  $10^{-15}$  indicating the accuracy with which the input moments can be matched with the reconstructed ones. A direct comparison with the exact functions studied here reveals that the method indeed converges to the correct solution provided a sufficient number of moments are available as input. The general trend of the convergence profile is similar in all the cases: the quality of the reconstructed function markedly improves with the increase in the number of moments. The numerical calculations suggest that the convergence toward the exact solution is almost of exponential nature.

## Acknowledgments

The work is partially supported by a fellowship from Aubrey Keith Lucas and Ella Ginn Lucas Endowment at the University of Southern Mississippi. PB would like to thank Lawrence Mead, David Drabold, and Roger Haydock for useful discussions during the course of the work.

- 
- [1] A. J. Shohat and J. D. Tamarkin, *The Problem of Moments* (American Mathematical Society, 1963)  
 [2] N. I. Akheizer, *The classical moment problem and some*

- related questions in analysis* (Hafner Publishing Co., New York, 1963)  
 [3] J. N. Kapur and H. K. Kesavan, *Entropy optimization*

and mathematical programming, Kluwer Academic Publishers, Dordrecht (1997)

- [4] A. Lent in *Image analysis and evaluation* (Edited by R. Shaw), SPSE, Washington, D.C (1953)
- [5] J. C. Wheeler and R.G. Gordon, *J. Chem. Phys.* **51**, 5566 (1969)
- [6] C. Isenberg, *Phys. Rev.* **150**, 712 (1966)
- [7] G. Bricogne, *Acta Cryst. A* **44**, 517 (1988)
- [8] C. J. Gilmore, *Acta Cryst. A* **52**, 561 (1996)
- [9] L.R. Mead and N. Papanicolaou, *J. Math. Phys.* **25**, 2404 (1984)
- [10] C.R. Smith and W.T. Grandy Jr., *Maximum entropy and Bayesian methods in inverse problems*, Reidel, Dordrecht (1985)
- [11] D. A. Drabold and O. F. Sankey, *Phys. Rev. Lett.* **70**, 3631 (1993)
- [12] A.E. Carlsson and P.A.Fedders, *Phy. Rev. B* **34**, 3567 (1986)
- [13] H. Gotovac and B. Gotovac, *J. Comp. Phys.* **228**, 9079 (2009)
- [14] F. Hausdorff, *Math. Z.* **16**, 220 (1923)
- [15] J. Hadamard, *Lectures on the Cauchy problem in linear partial differential equations*, Yale University Press, New Haven 1923
- [16] I. Turek, *J. Phys. C: Solid State Phys.* **21**, 3251 (1988)
- [17] A. Tikhonov and V. Y. Arsenine, *Solution of ill-posed problems*, V.H. Winston & Sons, Washington, D. C. (1977)
- [18] G.A. Viano, *J. Math. Anal. Appl.* **156**, 410 (1991)
- [19] E. Scalas and G. A. Viano, *J. Math. Phys.* **34**, 5781 (1993)
- [20] E.T. Jaynes, *Phys. Rev.* **106**, 620 (1957)
- [21] C. Shannon, *Bell Syst. Tech. J.* **27**, 379 (1948)
- [22] J-H. Schöfeldt, N. Jimenez, A.R. Plastino, A. Plastino and M. Casas, *Physica A* **374**, 573 (2007)
- [23] W-H. Steeb, F. Solms and R. Stoop, *J. Phys. A: Maths. Gen* **27**, L399 (1994)
- [24] A.A.Maradudin, E.W.Montroll, G.H.Weiss, and I.P.Ipatova, *Theory of lattice dynamics in harmonic approximation* (Academic Press, New York, 1971)
- [25] W.V. Houston, *Rev. Mod. Phys.* **20**, 161 (1948)
- [26] C. Domb and C. Isenberg, *Proc. Phys. Soc. London* **79**, 659 (1962)
- [27] R.N. Silver and H. Röder, *Phys. Rev. E* **56**, 4822 (1997)
- [28] K. Bandyopadhyay, A.K. Bhattacharya, P. Biswas and D.A. Drabold, *Phys. Rev. E* **71**, 057701 (2005)
- [29] S. Kullback, *Information theory and statistics* (Dover Publication, 1997)
- [30] A. Taglinai, *Appl. Math. and Comput.* **145**, 195 (2003)
- [31] J. Wimp, *Proc. Roy. Soc. Edinburgh* **82 A**, 273 (1989)
- [32] The solution is *least biased* as far as the entropy of the density function is concerned, and the Hausdorff conditions are satisfied. There is no guarantee that the maximum entropy solution would be close to the exact solution, particularly when the very first few moments are

used in the reconstruction procedure.

- [33] L. M. Bergman, *USSR Comput. Math. and Math. Phys.* **7**, 200 (1967)
- [34] The exact location of the abscissa is computed by linearly interpolating between the two ordinates that have zero and non-zero values. The accuracy (of the location of the abscissa) can be improved further by using more points in the quadrature formula.
- [35] C. Beck and F. Schlögl, *Thermodynamics of chaotic systems* (Cambridge University Press, Cambridge, United Kingdom, 1993)
- [36] R. Zwanzig, *Proc. Nat. Acad. Sci. USA* **85**, 2029 (1988)
- [37] J.M. Borwein, *SIAM J. Optim* **1**, 191 (1991)
- [38] G. T. Toussaint, *IEEE Trans. Inform. Theor.* **21**, 99 (1975)
- [39] S. Kullback, *IEEE Trans. Inform. Theor.* IT-13, 126 (1967)

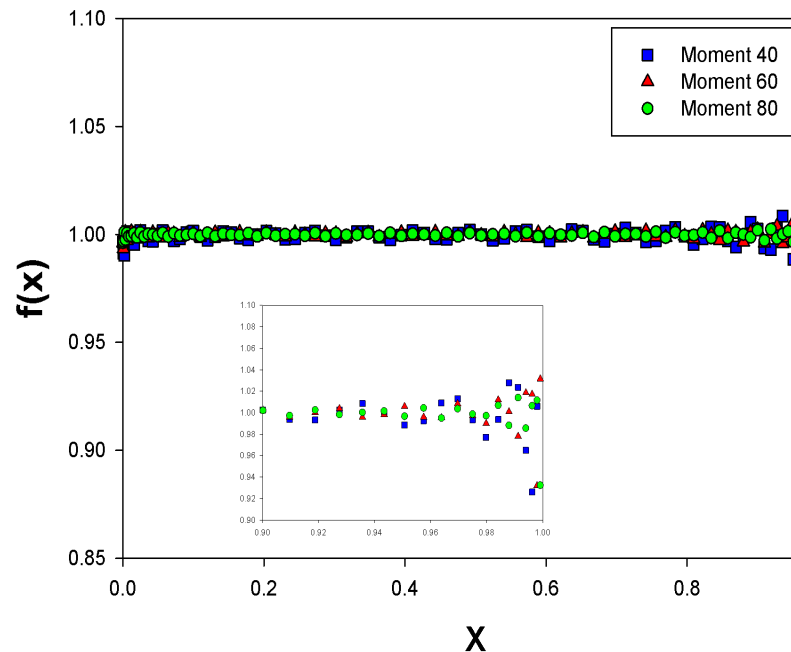


FIG. 1: (Color online) The step function,  $f(x) = 1$ , reconstructed using the first 40, 60, and 80 Chebyshev moments. The plot shows the presence of oscillations at the right edge with decaying amplitude as the number of moments increases. The data for 40, 60 and 80 moments are indicated in the figure by boxes (blue), triangles (red) and circles (green) respectively. A magnified view of the right edge is shown in the inset.



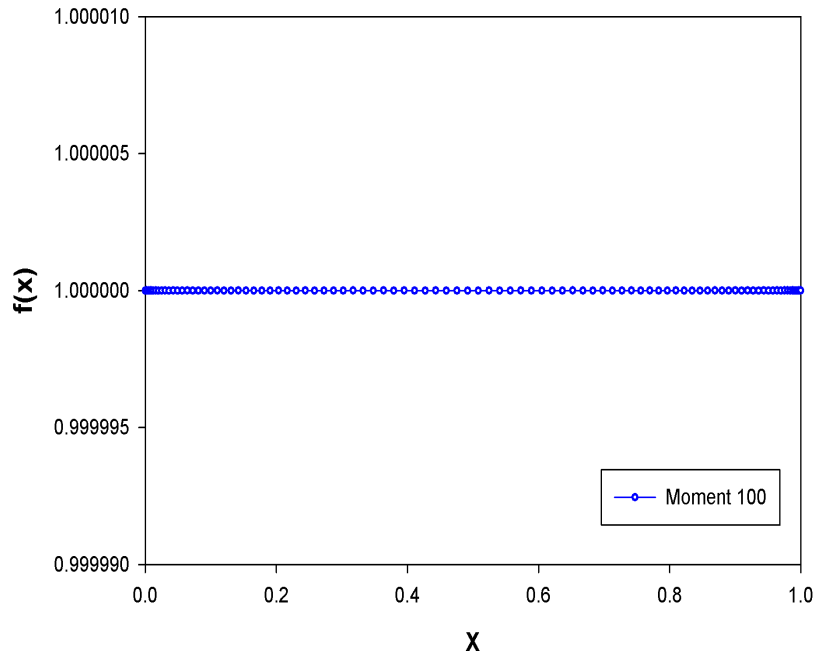


FIG. 2: (Color online) The step function as in fig.1 using the first 100 Chebyshev moments. The oscillations now completely disappear and the function is reproduced with an error less than 1 part in  $10^6$ .

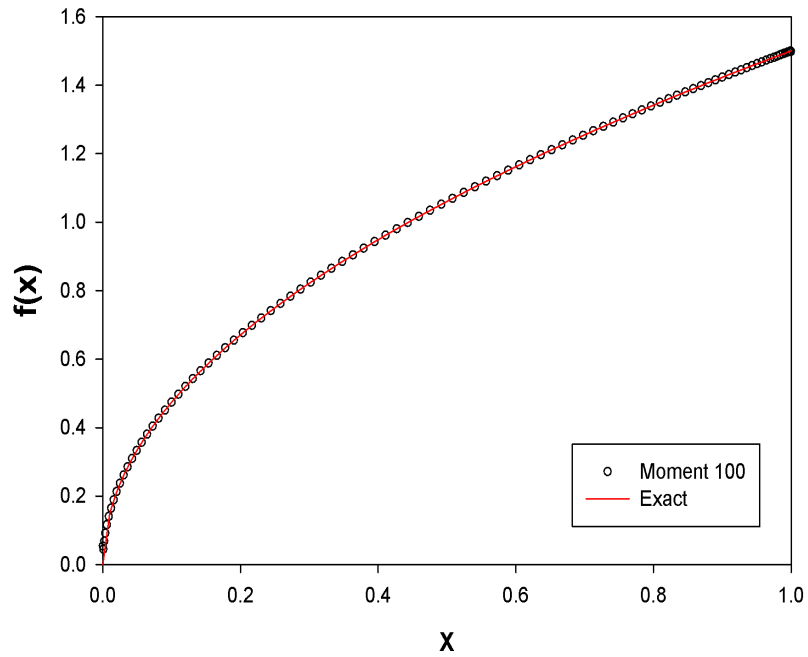


FIG. 3: The function,  $f(x) = \frac{3}{2}x^{\frac{1}{2}}$ , and its maximum entropy reconstruction using the first 100 Chebyshev moments. For clarity, every second data point is plotted in the figure. The exact function is evaluated at the quadrature points and is drawn as a line for comparison.

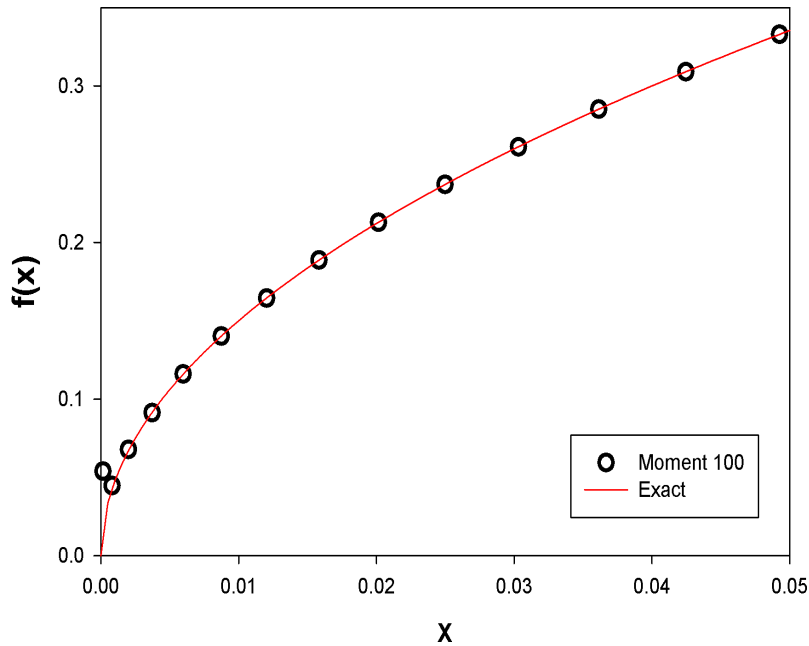


FIG. 4: The behavior of the function  $f(x) = \frac{3}{2}x^{\frac{1}{2}}$  for very small values of  $x$  along with the exact functional values evaluated at the quadrature points. Note that only one point is off the graph indicating an excellent match to the exact function for 100 moments.

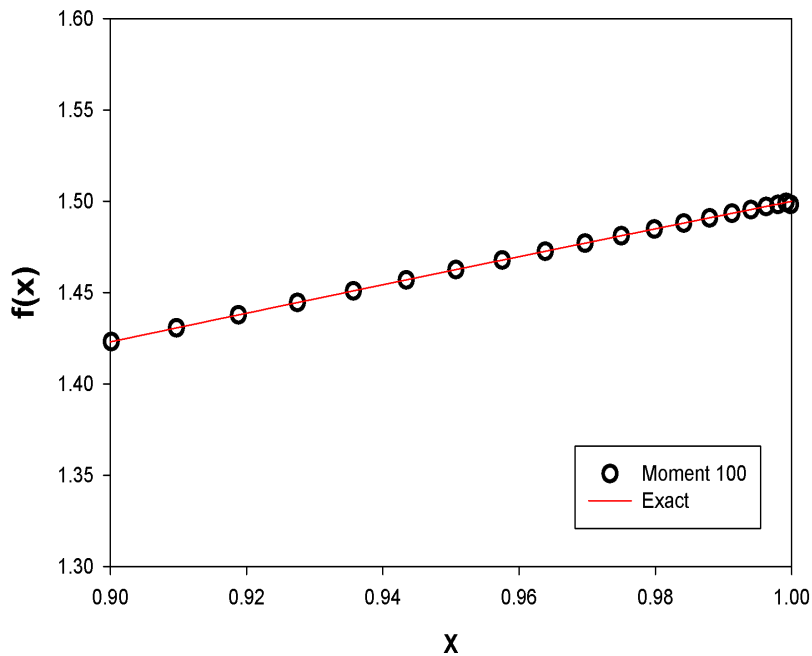


FIG. 5: The behavior of the function  $f(x) = \frac{3}{2}x^{\frac{1}{2}}$  near  $x = 1$ . The exact function is also plotted for comparison.

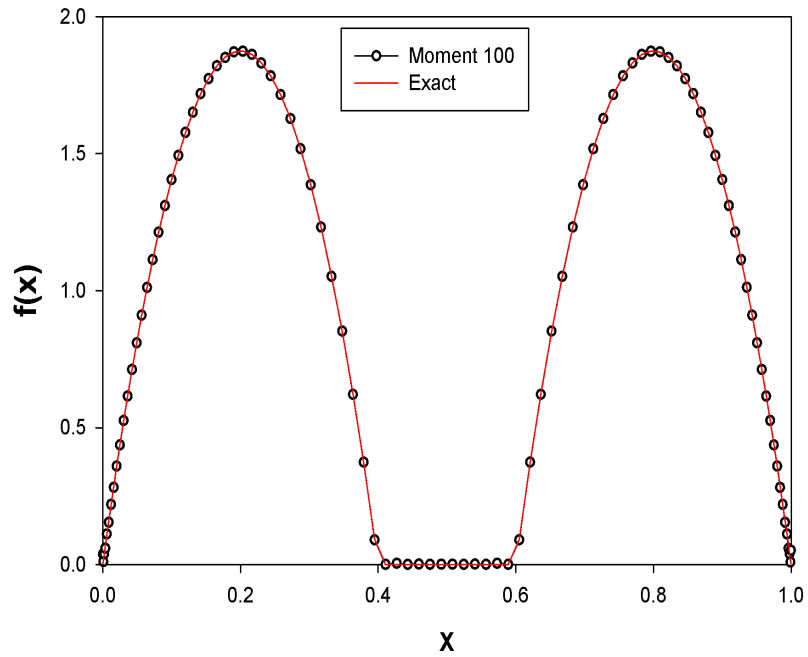


FIG. 6: The reconstruction of a function with a gap in the interval. The double-parabola with a gap is reconstructed using the first 100 moments. The exact values are also plotted in the figure for comparison.

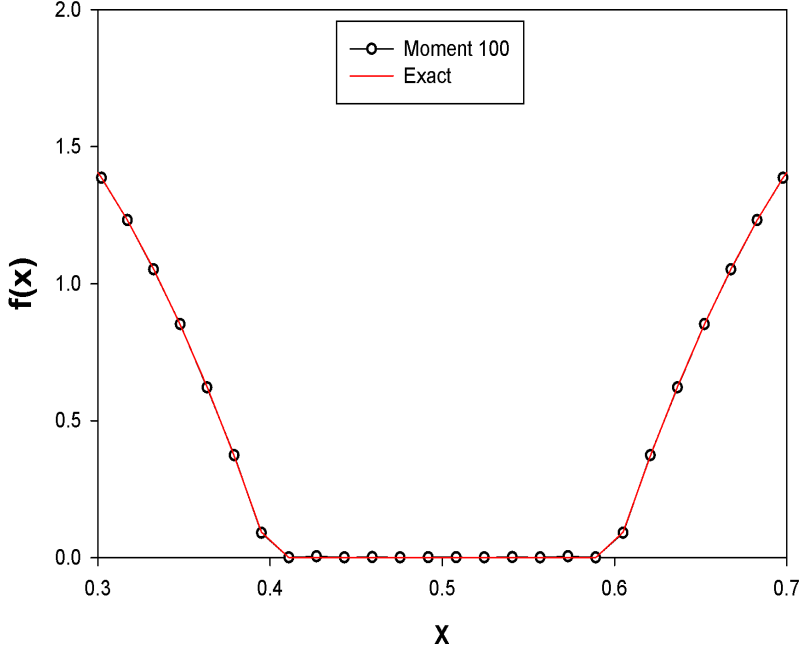


FIG. 7: The reconstructed double-parabola near the gap along with the exact function at the quadrature points. Owing to the finite number of quadrature points, the reconstructed function has a non-zero value at  $x_1 = 0.4$  and  $x_2 = 0.6$ .

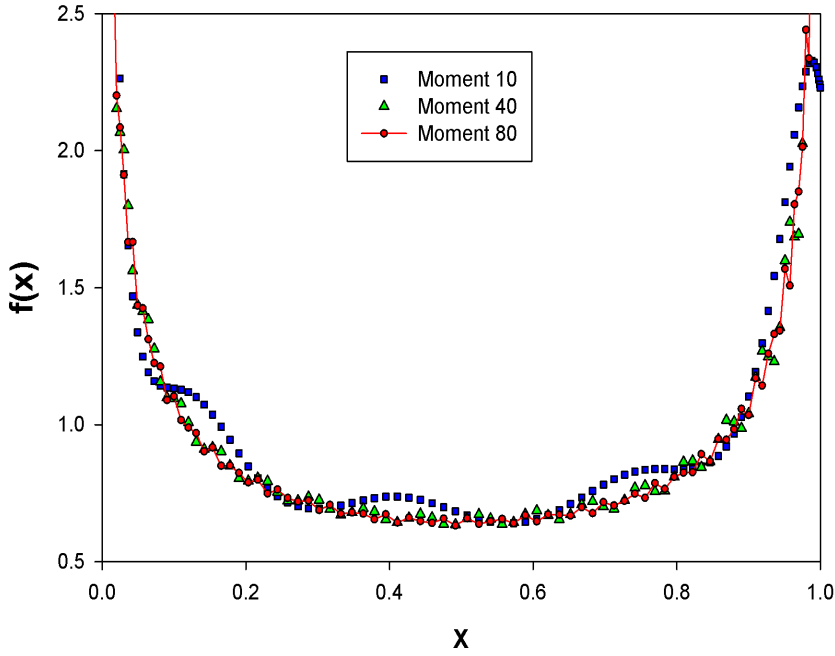


FIG. 8: (Color online) Reconstruction of the U-function as defined in the text. The data correspond to the first 10, 40 and 80 moments as indicated in the plot.

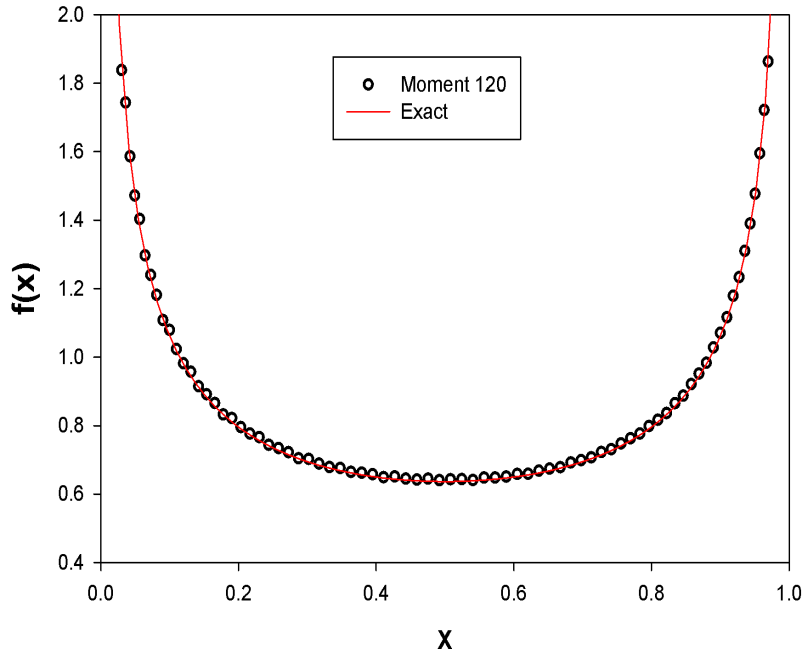


FIG. 9: The reconstructed U-function using the first 120 moments along with the exact function evaluated at the quadrature points. The reconstructed function matches point-wise to the functional values as indicated in the figure.

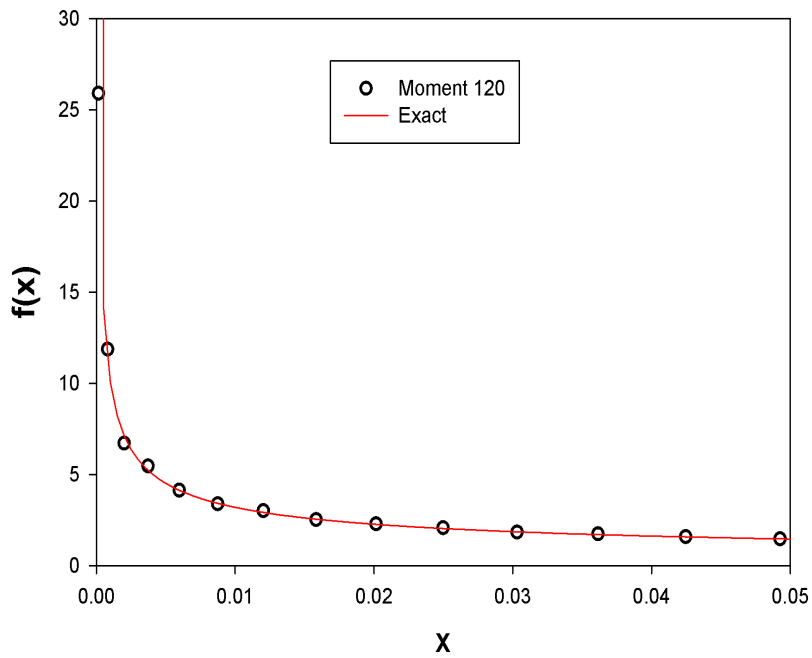


FIG. 10: The divergent behavior of the U-function near  $x = 0$ . The method accurately reproduces the function for very small values of  $x$ .

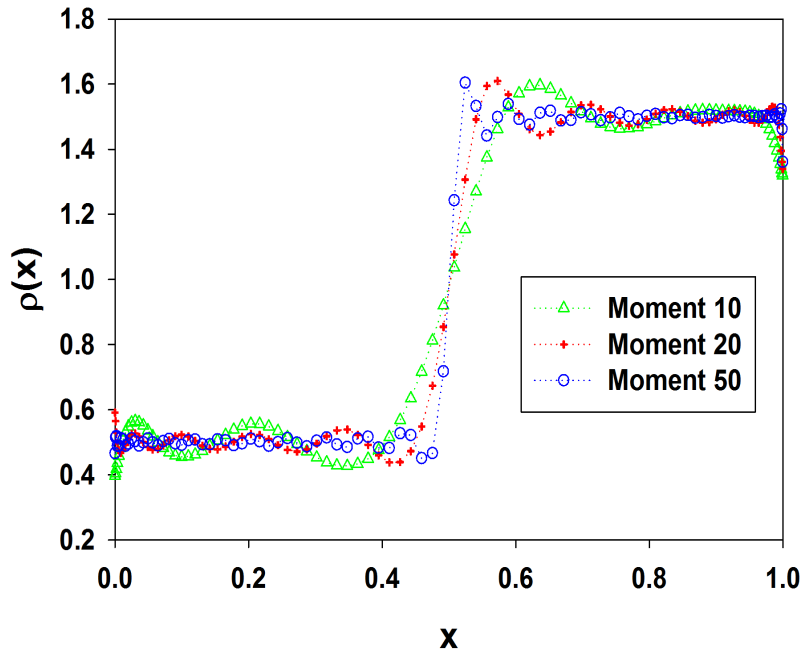


FIG. 11: (Color online) The reconstructed double-step function for the first 10, 20 and 50 moments. The reconstructed function improves progressively with the increase in the number of moments.

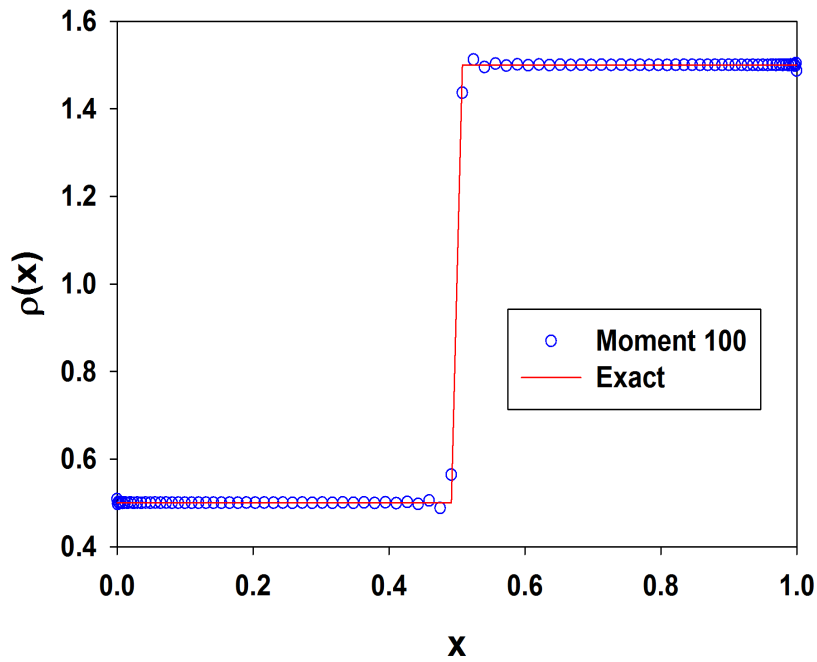


FIG. 12: (Color online) The reconstructed double-step function using the first 100 moments. The exact function is also shown as a line.

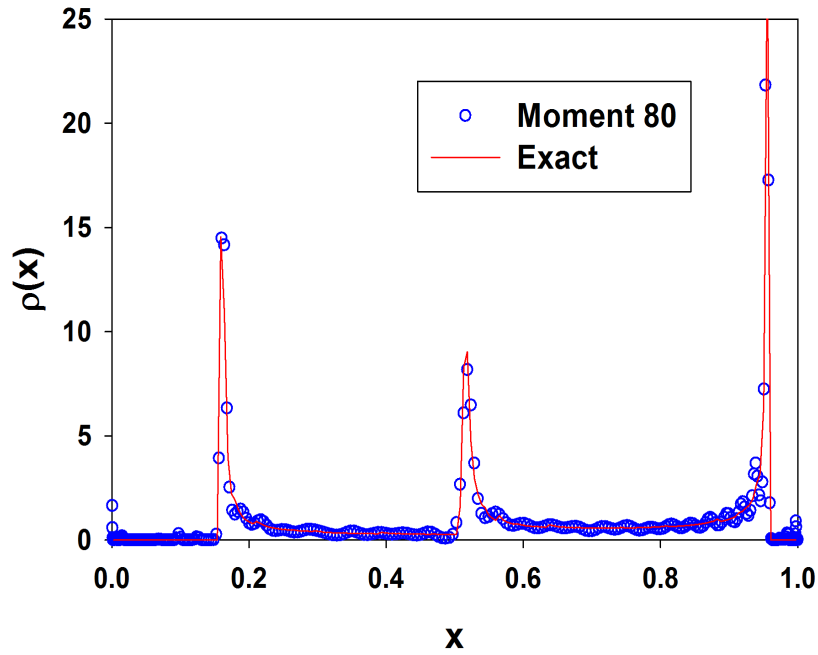


FIG. 13: A reconstructed density with sharp peaks obtained from the first 80 moments. The distribution corresponds to the natural invariant density of the logistic map as discussed in the text. The line corresponds to the numerical density obtained via histogram method.



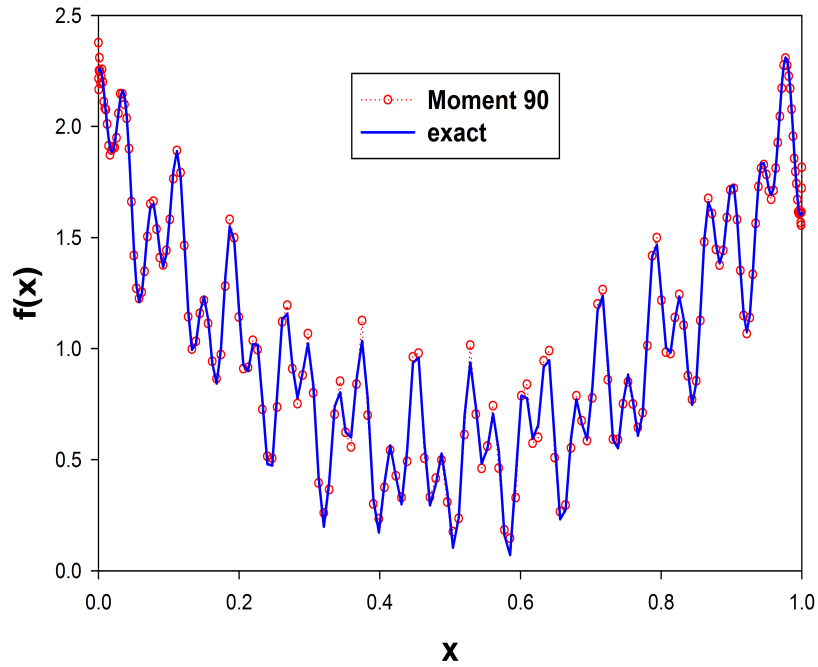


FIG. 14: (Color online) The reconstruction of an oscillatory function with a fine structure as discussed in the text. The exact functional values are also plotted at the quadrature points for comparison. The location of the local minima and maxima are excellently reproduced from the first 90 moments of the function.

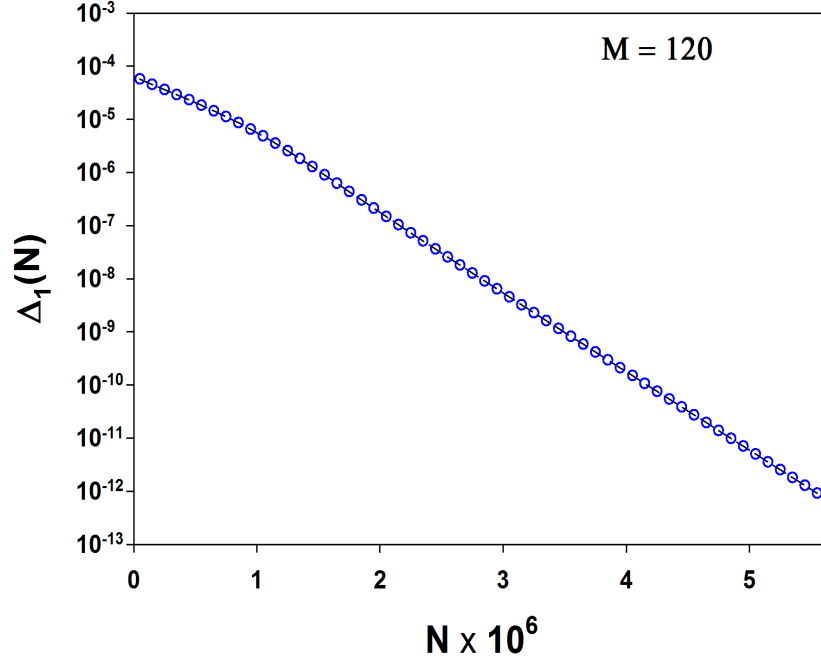


FIG. 15: The semi-log plot of the RMS deviation  $\Delta_1(N)$  for the U-function with iteration  $N$  expressed in unit of  $10^6$ . The RMS values decay exponentially with iteration after an initial crossover around  $N = 0.8$ . For clarity of presentation, every second data point is plotted in the figure. The number of moments is indicated in the figure.

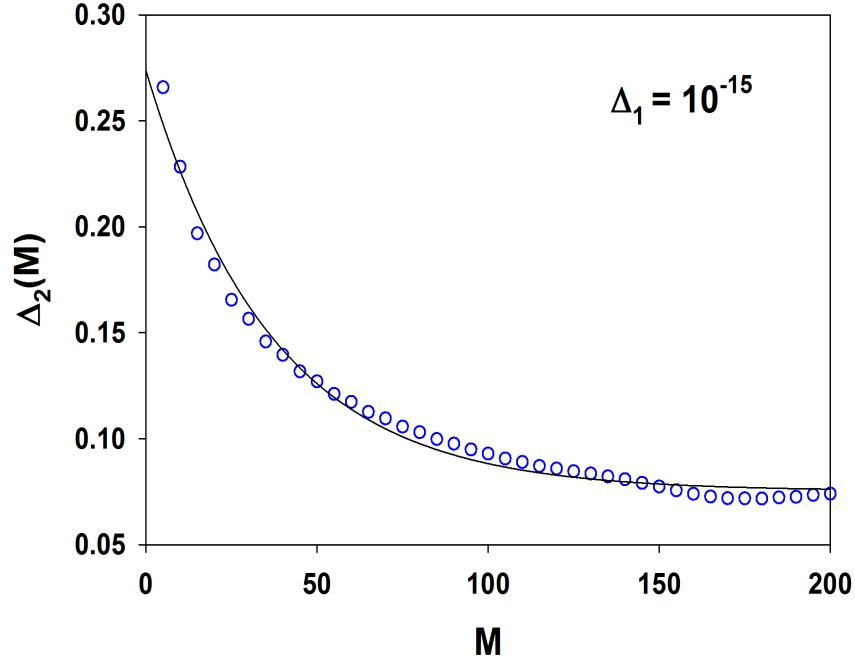


FIG. 16: The variation of the RMS deviation  $\Delta_2(M)$  with moments for a given value of  $\Delta_1 = 10^{-15}$ . The data can be fitted to exponential decay as indicated by the best fitted line in the plot.

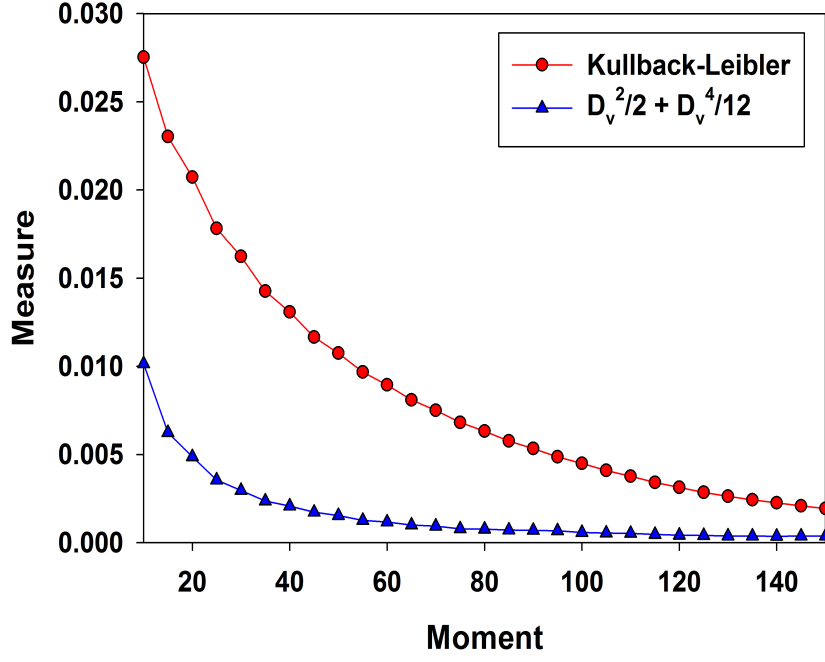


FIG. 17: The variation of the KL divergence measure (circles) of the U-function for different number of moments. The function of the variation measure from the right hand side of the inequality (11) is also plotted for comparison. The data correspond to the reconstructed solution with  $\Delta_1 = 10^{-15}$ .